

See discussions, stats, and author profiles for this publication at: <https://www.researchgate.net/publication/244405239>

Adsorption of Polymeric Lattice Fluids at a Noninteracting Hard Wall: A Comparison of Discretized Polymer–Reference Interaction Site Model (RISM) Theory, Scheutjens–Fleer Theory, a...

ARTICLE *in* LANGMUIR · MAY 1997

Impact Factor: 4.46 · DOI: 10.1021/la9608932

CITATIONS

8

READS

6

3 AUTHORS, INCLUDING:



Erik Nies

University of Leuven

78 PUBLICATIONS 951 CITATIONS

SEE PROFILE



Peter Cifra

Slovak Academy of Sciences

96 PUBLICATIONS 1,025 CITATIONS

SEE PROFILE

Adsorption of Polymeric Lattice Fluids at a Noninteracting Hard Wall: A Comparison of Discretized Polymer-Reference Interaction Site Model (RISM) Theory, Scheutjens–Fleer Theory, and Monte Carlo Simulations

R. H. C. Janssen and E. Nies*

Department of Polymer Technology, Eindhoven University of Technology, P.O. Box 513,
5600 MB Eindhoven, The Netherlands

P. Cifra

Polymer Institute, Slovak Academy of Sciences, 842 36 Bratislava, Slovakia

Received September 16, 1996. In Final Form: March 4, 1997[®]

A discretized version of the polymer-reference interaction site model (RISM) theory is investigated on its capabilities to assess the adsorption behavior of interacting polymeric lattice fluids near a flat wall. Both the density profile of the fluid at the wall and the equation of state of the bulk fluid (obtained from the density profile via a method of Dickman) are compared to Monte Carlo simulations. The profiles are also compared to the outcome of a classical lattice-based adsorption theory, the Scheutjens–Fleer formalism. At all bulk packing fractions, the Scheutjens–Fleer theory is found to be superior to the polymer-RISM theory, although it is made plausible that the performance of the discretized polymer-RISM theory can be improved significantly by using a nonreversal random walk intramolecular distribution, instead of the random walk intramolecular distribution used in this work.

1. Introduction

Polymer adsorption is an interesting phenomenon with wide applications in, e.g., the composite and coatings industry. An understanding of the molecular origins of the adsorption phenomenon is of importance in optimizing processes in these industries.

Classical approaches to study polymer adsorption build on work performed on bulk lattice^{1,2} and continuum fluids.^{3,4} Well-known lattice-based adsorption theories are those of Helfand^{5,6} and Scheutjens and Fleer.^{7–9} An important aspect of these theories is that they account for the changes in conformational entropy of the molecules in the interfacial region. Well-known theories that consider the adsorption of a continuum space polymeric fluid at a solid wall are the theories of Helfand¹⁰ and Hong and Noolandi.¹¹ These continuum approaches use Gaussian random walk (GRW) chain statistics to describe the polymer chain conformations in the interfacial region. GRW chain statistics apply in the bulk of dense one-component fluids¹² but are not suited for situations that deviate strongly from the bulk circumstances. Hence, the theories of refs 10 and 11 are less suited in cases where strong wall–fluid interactions cause the interfacial region to be very different from the bulk of the fluid.

In this paper we investigate an approach to the polymer adsorption phenomenon that does not build on the work of refs 1–4. It is based on integral equations that describe the correlations of the fluid particles with the adsorbing wall. Work along this line has been presented previously in refs 13–16 in which the adsorption of monatomic spherical particles was considered. Only the integral equation study of Yethiraj and Hall¹⁷ considered the adsorption of large flexible polymeric molecules. Their method to calculate the adsorption profiles of a continuum space polymeric fluid near a solid impenetrable wall is based on the polymer-RISM theory.^{18,19} This theory is primarily designed to explain the packing effects present in dense continuum space fluids. Yethiraj and Hall indeed found that their predictions for athermal systems are in excellent agreement with Monte Carlo (MC) simulations provided the bulk density was high enough to dominate the ordering of the fluid near the wall, i.e., in the absence of a depletion layer. In the case where depletion is important, i.e., for high molecular weight fluids or at lower bulk density, better results for the adsorption profiles are obtained via the off-lattice self-consistent field (SCF) theory of Björling and Linse.²⁰ However, this SCF theory only captures qualitatively the layering (“packing”) that occurs at high densities.

In the work presented here we apply the method of Yethiraj and Hall to calculate the adsorption profiles, i.e., the fluid density as a function of distance from the wall, of a cubic lattice fluid. This allows for direct comparison to the results obtained with a classical SCF lattice model, the Scheutjens–Fleer adsorption theory.⁷ Furthermore, we have compared the profiles to Monte Carlo simulation data at constant number of particles, pressure, and

* Author to whom correspondence should be addressed.

[®] Abstract published in *Advance ACS Abstracts*, April 15, 1997.

(1) Flory, P. J. *Principles of Polymer Chemistry*; Cornell University Press: Ithaca, NY, 1953.

(2) Huggins, M. L. *J. Chem. Phys.* **1941**, *9*, 440.

(3) Edwards, S. F. *Proc. Phys. Soc. London* **1965**, *85*, 613.

(4) Freed, K. F. *Renormalization Group Theory of Macromolecules*; Wiley-Interscience: New York, 1987.

(5) Helfand, E. *J. Chem. Phys.* **1975**, *63*, 2192.

(6) Helfand, E. *Macromolecules* **1976**, *9*, 307.

(7) Scheutjens, J. M. H. M.; Fleer, G. J. *J. Phys. Chem.* **1979**, *83*, 1619.

(8) Theodorou, D. N. *Macromolecules* **1988**, *21*, 1400.

(9) Evers, O. A. Statistical Thermodynamics of Block Copolymer Adsorption. Ph.D. Thesis, Wageningen Agricultural University, Wageningen, The Netherlands, 1993.

(10) Helfand, E. *J. Chem. Phys.* **1975**, *62*, 999.

(11) Hong, K. M.; Noolandi, J. *Macromolecules* **1981**, *14*, 1229.

(12) Flory, P. J. *J. Chem. Phys.* **1949**, *17*, 303.

(13) Henderson, D.; Abraham, F. F.; Barker, J. A. *Mol. Phys.* **1976**, *31*, 1291.

(14) Henderson, D.; Plischke, M. *J. Phys. Chem.* **1988**, *92*, 7177.

(15) Zhou, Y.; Stell, G. *J. Chem. Phys.* **1988**, *89*, 7010.

(16) Schlijper, A. G.; Smit, B. *Fluid Phase Equilib.* **1992**, *76*, 11.

(17) Yethiraj, A.; Hall, C. K. *J. Chem. Phys.* **1991**, *95*, 3749.

(18) Schweizer, K. S.; Curro, J. G. *Phys. Rev. Lett.* **1987**, *58*, 246.

(19) Chandler, D.; Andersen, H. C. *J. Chem. Phys.* **1972**, *57*, 1930.

(20) Björling, M.; Linse, P. *J. Chem. Phys.* **1992**, *97*, 6890.

temperature (NpT). We have also used the adsorption profiles obtained with the integral equation formalism to obtain an equation of state (EoS) of the bulk fluid via a method of Dickman.²¹ The results for the EoS are also compared to simulation data.

The outline of the rest of this paper is as follows. In section 2.1 the method of Henderson, Abraham, and Barker (HAB)¹³ for introducing a flat wall in an integral equation formalism is applied to a discretized version of the polymer-RISM equation. The HAB method is particularly easy to employ in our case of a cubic lattice fluid. The principal results of section 2.1 are expressions for the adsorption profiles and isotherms of a one-component polymeric lattice fluid consisting of linear chains. In section 2.2 the solution procedure is briefly outlined. It is particularly easy to employ and boils down to solving two equations in two unknowns via a Newton–Raphson scheme. In section 2.3 we very briefly recapitulate a method developed by Dickman to extract an EoS of the bulk lattice fluid from the adsorption profiles. In section 3 the NpT -MC simulation is briefly considered. Thus far, we only performed simulations for 30-mers at a noninteracting wall. Fluids with segmental interaction energies of $u_{\text{attr}} = -0.0k_B T$ and $-0.2k_B T$ have been considered. The adsorption profiles that are obtained from the simulations were extracted from runs previously used to assess the bulk structural and EoS properties of the polymeric lattice fluids.^{22,23} In section 4 the results for the adsorption profiles and EoS are presented, compared, and discussed. Conclusions are collected in section 5.

2. Polymer-RISM Theory for Lattice Fluids near a Solid Wall

2.1. Outline of the Method. In this section the discretized version of the polymer-reference interaction site model (RISM) equation,²⁴ considered previously in refs 22 and 23, is modified to enable the calculation of the adsorption profiles of polymeric lattice fluids at an impenetrable wall. The method¹³ was originally used to study the behavior of a simple continuum fluid near an impenetrable wall and was later applied to study adsorption within the polymer-RISM theory.¹⁷ The general principle of the method is as follows. First, the polymer-RISM equation for a mixture of two molecule types, simple monatomic particles and polymeric molecules, is written down. Secondly, the concentration of the simple fluid particles is reduced to zero to ensure that these particles do not influence each other. In a last step, the simple particles are extended in two directions such that they turn into a wall. Then, construction of the adsorption profile of the polymer molecules at the wall amounts to calculating the correlations between the wall and an average polymer segment. From the adsorption profile the amount of adsorbed material can be quantified by construction of an adsorption isotherm. Consider a mixture of two particle types, simple monatomic particles that occupy exactly one lattice site and linear polymer chains. The chains consist of s covalently bonded segments that occupy consecutive sites on a cubic lattice. The monatomic particles and the segments of the polymer molecules interact via nearest neighbor potentials given by

$$u_{ij}(0,0,0) \rightarrow \infty$$

$$u_{ij}(l,m,n) = u_{\text{attr},ij} \quad \text{if } l^2 + m^2 + n^2 = 1$$

$$u_{ij}(l,m,n) = 0 \quad \text{otherwise} \quad (1)$$

where $\{i,j\} \in \{1,2\}$ denote the particle type: $i = 1$ corresponds to a monatomic particle and $i = 2$ to a segment of a polymer chain. The structural correlations present in such a mixture can be studied with the polymer-RISM equation for mixtures. It can conveniently be written down in matrix form, and on the 3D cubic lattice it is given by^{18,22}

$$\hat{\mathbf{H}}(u,v,w) = \hat{\Omega}(u,v,w)\hat{\mathbf{C}}(u,v,w)(\hat{\Omega}(u,v,w) + \hat{\mathbf{H}}(u,v,w)) \quad (2)$$

in which $\hat{\mathbf{H}}$, $\hat{\Omega}$, and $\hat{\mathbf{C}}$, are 2×2 matrices with elements $\eta_{m1}\eta_{mj}\hat{h}_{ij}(u,v,w)$, $\eta_{m1}\delta_{ij}\hat{\omega}_i(u,v,w)$, and $\hat{c}_{ij}(u,v,w)$. The symbols η_{m1} and η_{m2} denote respectively the packing fractions of monatomic particles and of the segments of the polymeric molecules. The Kronecker delta, δ_{ij} , has a value 1 if $i = j$ and 0 otherwise. The $\hat{h}_{ij}(u,v,w)$, $\hat{\omega}_i(u,v,w)$, and $\hat{c}_{ij}(u,v,w)$ represent respectively the total intermolecular two-particle correlation function, the intramolecular two-particle distribution, and the direct correlation function.¹⁸ The $\hat{h}_{ij}(u,v,w)$, $\hat{c}_{ij}(u,v,w)$, and $\hat{\omega}_i(u,v,w)$ are written in 3D Fourier space, defined by

$$\hat{f}(u,v,w) = \sum_{l,m,n} f(l,m,n) \cos lu \cos mv \cos nw \quad (3)$$

with $f = h, \omega$, or c . equation 3 is only valid if the symmetry conditions $f(l,m,n) = f(\pm l, \pm m, \pm n)$ apply. The real space analogs of $\hat{h}_{ij}(u,v,w)$, $\hat{\omega}_i(u,v,w)$, and $\hat{c}_{ij}(u,v,w)$ can be found via inverse transformation

$$f(l,m,n) = \left(\frac{1}{2\pi}\right)^3 \int_{-\pi}^{\pi} \int_{-\pi}^{\pi} \int_{-\pi}^{\pi} \hat{f}(u,v,w) \times \cos lu \cos mv \cos nw \, du \, dv \, dw \quad (4)$$

The meaning of the real space direct correlation function, $c_{ij}(l,m,n)$, is merely mathematical, in contrast with $h_{ij}(l,m,n)$ and $\omega_i(l,m,n)$. The total intermolecular correlation function, $h_{ij}(l,m,n)$, is related to the probability $P_{ij}(l,m,n)$ of finding a particle j at distance (l,m,n) from another particle i that is part of a different molecule, via $P_{ij}(l,m,n) = \eta_{mj} (h_{ij}(l,m,n) + 1)$. The $\omega_i(l,m,n)$ is the intramolecular two-particle distribution function. For the monatomic particles the only nonzero term is $\omega_1(0,0,0) = 1$, but in the case of flexible polymer molecules $\omega_2(l,m,n)$ does give the packing fraction of segments located at (l,m,n) from an average segment belonging to the same molecule. If the polymer molecules are considered to be random flights, which is a reasonable first approximation,^{12,24} then $\hat{\omega}_2(u,v,w)$ is given by^{22,25,26}

$$\hat{\omega}_{2,\text{RF}}(u,v,w) = \frac{1 - \hat{\tau}^2 - \frac{2}{5}\hat{\tau} + \frac{2}{5}\hat{\tau}^{s+1}}{(1 - \hat{\tau})^2} \quad (5)$$

in which $\hat{\tau}(u,v,w) = (\cos u + \cos v + \cos w)/3$ is the Fourier transform, eq 3, of the one-jump probability

$$\tau(l,m,n) = \frac{1}{6} \quad \text{if } l^2 + m^2 + n^2 = 1$$

(21) Dickman, R. *J. Chem. Phys.* **1987**, *87*, 2246.
(22) Janssen, R. H. C.; Nies, E.; Cifra, P. Submitted for publication in *Macromolecules*.

(23) Janssen, R. H. C. Structure and Thermodynamics of lattice fluids in Bulk and at Interfaces. Ph.D. Thesis, Eindhoven University of Technology, Eindhoven, The Netherlands, 1996.

(24) Curro, J. G.; Schweizer, K. S. *Macromolecules* **1987**, *20*, 1928.

(25) Chandrasekhar, S. *Rev. Mod. Phys.* **1943**, *15*, 1.

(26) Cummings, P. T.; Stell, G. *J. Stat. Phys.* **1983**, *33*, 709.

$$\tau(l, m, n) = 0 \quad \text{otherwise} \quad (6)$$

From eq 6 it is clear that only jumps between nearest neighbor sites are allowed in our model. The discretized polymer-RISM equation eq 2 can be used to study the structural properties of polymer mixtures on a cubic lattice if the monatomic particles 1 are replaced by a second type of polymer molecules (see, e.g., refs 18 and 27–30), but in this work eq 2 is used to study the **adsorption** of a polymeric lattice fluid at a flat wall. For that purpose we perform the matrix multiplications in eq 2 and take the limit $\eta_{m1} \rightarrow 0$. A set of four equations results. It is given by

$$\hat{h}_{ij}(u, v, w) = \hat{\omega}_i(u, v, w) \hat{c}_{ij}(u, v, w) \hat{\omega}_j(u, v, w) + \eta_{m2} \hat{\omega}_i(u, v, w) \hat{c}_{i2}(u, v, w) \hat{h}_{2j}(u, v, w) \quad (7)$$

for $\{i, j\} \in \{1, 2\}$. The particles of type 1 are monomers, thus from $\omega_1(0, 0, 0) = 1$ and eq 3, we have $\hat{\omega}_1(u, v, w) = 1$. For $ij = 11$, eq 7 describes the correlations between the simple fluid particles in the mixture. This is of no interest to us here: the concentration of simple fluid particles η_{m1} was reduced to zero to exclude encounters of such particles, which guarantees that the other correlations in the mixture are independent of the correlations between the simple fluid particles. For $ij = 12$ or 21 eq 7 denotes the correlations between a simple fluid particle and a polymer segment, and finally, for $ij = 22$ eq 7 governs the correlations occurring between two average segments of two different polymer molecules. In that case eq 7 is identical to the discretized polymer-RISM equation.^{22–24} It determines the bulk structural properties of the polymeric molecules of type 2 and can be solved separately from the three other equations in eq 7 along the lines presented in refs 22 and 23. The results for the bulk structural quantities of the polymeric fluid, \hat{h}_{22} , \hat{c}_{22} and $\hat{\omega}_2$, are subsequently used as input quantities in the calculation of the adsorption profile of the polymeric fluid from eq 7 with $ij = 12$. (Alternatively we can also take $ij = 21$.) Equation 7 (with $ij = 12$) is written in real space form with the help of eq 4 as

$$h_{12}(l, m, n) = \sum_{l', m', n'} (\omega_2(l', m', n') + \eta_{m2} h_{22}(l', m', n')) c_{12}(l - l', m - m', n - n') \quad (8)$$

The monatomic particle 1 can now effectively be extended in m and n direction by removing the m and n coordinates in the arguments of $h_{12}(l, m, n)$ and $c_{12}(l, m, n)$: only the l distance to particle 1 remains to be a positional parameter, and therefore, the particle turns into a wall.¹³ Hence, from eq 8 we obtain

$$h_{12}(l) = \sum_{l', m', n'} (\omega_2(l', m', n') + \eta_{m2} h_{22}(l', m', n')) c_{12}(l - l') \quad (9)$$

Note that the creation of a wall is particularly easy on the cubic lattice, which is due to the independence of l , m , and n . eq 9 is the discretized version of the equation that was used in ref 17 to study the adsorption behavior of continuum space polymeric fluids. To obtain the distribution of an average polymer segment with respect to the wall, eq 9 has to be combined with a closure equation. Here we apply the Percus–Yevick closure. In 1D form it

is given by³¹

$$g_{12}(0) = 0$$

$$c_{12}(l) = g_{12}(l)(1 - e^{\beta u_{12}(l)}) \quad l \geq 1 \quad (10)$$

where $u_{12}(l)$ is the wall–fluid interaction potential. It is given by eq 1 for $i = 1$ and $j = 2$ upon removal of the m and n dependence in that equation. Note that the wall–fluid interaction is of nearest neighbor type. In eq 10, $g_{12}(l)$ denotes the segmental distribution with respect to the wall. Its calculation is the objective of the work presented here. The $g_{12}(l)$ and $h_{12}(l)$ are related as

$$h_{12}(l) = g_{12}(l) - 1 \quad (11)$$

From the adsorption profile of the polymeric lattice fluid, $\eta_{m2} g_{12}(l)$, an adsorption isotherm, $\Gamma(\eta_{m2})$, is constructed as

$$\Gamma(\eta_{m2}) = \sum_{l=1}^{l_{\text{bulk}}} \eta_{m2} h_{12}(l) \quad (12)$$

where l_{bulk} is taken sufficiently large for the summation to reach into the bulk region of the polymeric fluid. Note that $\eta_{m2} h_{12}(l)$ is the excess amount of adsorbed material relative to the bulk.

The method presented in this section is also suitable to study competitive adsorption for two or more molecule types.³² In that case the number of molecule types in the matrix of eq 2 has to be extended, but the general procedure is not changed. Here we are only interested in a first test of the lattice formalism and we have only studied one-component fluids consisting of linear polymer chains.

2.2. Solution procedure. Equations 9–11 form a complete set of equations from which the adsorption profile, $\eta_{m2} g_{12}(l)$, and adsorption isotherm, $\Gamma(\eta_{m2})$, can be constructed if the bulk structural properties of the polymeric fluid, $\hat{h}_{22}(u, v, w)$ and $\hat{\omega}_2(u, v, w)$, are known. These quantities have already been obtained in refs 22 and 23.

The set of eqs 9–11 are conveniently solved in 1D-Fourier space, defined by

$$\tilde{f}(u) = \sum_l f(l) \cos lu \quad (13)$$

with inverse

$$f(l) = \frac{1}{2\pi} \int_{-\pi}^{\pi} \tilde{f}(u) \cos lu \, du \quad (14)$$

With help of eq 13 we can write eq 9 as

$$\tilde{h}_{12}(u) = (\hat{\omega}_2(u, 0, 0) + \eta_{m2} \hat{h}_{22}(u, 0, 0)) \tilde{c}_{12}(u) \quad (15)$$

where $\hat{h}_{22}(u, 0, 0)$ and $\hat{\omega}_2(u, 0, 0)$ are 3D-Fourier series, given by Eq 3 for $v = w = 0$. We do not have to take Fourier sine terms into account in eq 13, because blowing up particle 1 does not violate the symmetry relation $h_{12}(l) = h_{12}(-l)$. In eq 15 we replace $\hat{\omega}_2(u, 0, 0) + \eta_{m2} \hat{h}_{22}(u, 0, 0)$ by $\hat{\omega}_2(u, 0, 0)/(1 - \eta_{m2} \hat{\omega}_2(u, 0, 0) \hat{c}_{22}(u, 0, 0))$ (see eq 7 for $ij = 22$), which is convenient due to the short-ranged character of the direct correlation function $\hat{c}_{22}(u, v, w)$. Combination of eq 15 with the 1D-PY closure, eq 10, thus results in two equations in the unknowns $c_{12}(0)$ and $c_{12}(1)$

(27) Schweizer, K. S.; Curro, J. G. *J. Chem. Phys.* **1989**, *91*, 5069.

(28) Curro, J. G.; Schweizer, K. S. *Macromolecules* **1991**, *24*, 6736.

(29) Schweizer, K. S.; Yethiraj, A. *J. Chem. Phys.* **1993**, *98*, 9053.

(30) Honeycutt, J. D. *Macromolecules* **1994**, *27*, 5377.

(31) Percus, J. K.; Yevick, G. J. *Phys. Rev.* **1958**, *110*, 1.

(32) Yethiraj, A. *Phys. Rev. Lett.* **1995**, *74*, 2018.

$$-1 = \frac{1}{2\pi} \int_{-\pi}^{\pi} \frac{\hat{w}_2(u,0,0)}{1 - \eta_{m2} \hat{w}_2(u,0,0) \hat{c}_{22}(u,0,0)} \tilde{c}_{12}(u) du$$

$$c_{12}(1)/(1 - e^{\beta u_{12}(1)}) - 1 = \frac{1}{2\pi} \int_{-\pi}^{\pi} \frac{\hat{w}_2(u,0,0)}{1 - \eta_{m2} \hat{w}_2(u,0,0) \hat{c}_{22}(u,0,0)} \tilde{c}_{12}(u) \cos u du \quad (16)$$

in which, from eqs 10 and 13, $\tilde{c}_{12}(u) = c_{12}(0) + 2c_{12}(1) \cos u$. Equation 16 is solved numerically with a combined Newton–Raphson 1D quadrature routine. Once $c_{12}(0)$ and $c_{12}(1)$ are found, the wall-segment correlations are obtained from

$$h_{12}(l) = \frac{1}{2\pi} \int_{-\pi}^{\pi} \frac{\hat{w}_2(u,0,0)}{1 - \eta_{m2} \hat{w}_2(u,0,0) \hat{c}_{22}(u,0,0)} \tilde{c}_{12}(u) \cos lu du \quad (17)$$

(See eqs 14 and 15.)

From eq 16, the adsorption profile of an athermal monomeric fluid is found to be

$$h_{12}(0) = -1$$

$$h_{12}(1) = - \left(\frac{(\eta_{m2} - 1)(1 - e^{\beta u_{12}(1)})}{1 + (\eta_{m2} - 1)(1 - e^{\beta u_{12}(1)})} \right)$$

$$h_{12}(l) = 0 \quad \text{if } l \geq 2 \quad (18)$$

It can be shown that this result is exact.²³ Note from eq 18 that the influence of the wall reaches only one layer deep into the athermal monomeric fluid.

2.3. The Wall Equation of State. Dickman^{21,33} has presented a method to calculate the EoS of a polymeric lattice fluid from its adsorption profile at a repulsive wall. It is an alternative to the pressure route^{34,35} which is not valid for lattice fluids.²¹ The lattice wall EoS reads

$$\frac{Pv_0}{k_B T} = \int_{\phi=0}^1 \frac{\eta_{m2} g_{12}(l)}{\phi} d\phi \quad (19)$$

where v_0 is the volume of one lattice site and $\phi = e^{-\beta u_{12}(1)}$. In the derivation of eq 19, the overall potential energy of the system is divided in a bulk part containing the restrictions which define the chain connectivity and prohibit segmental overlaps, and in a part U_{12} caused by the wall–fluid interactions. If U_{12} is further decomposed (which is possible without approximation) into separate nearest neighbor wall-segment interactions $u_{12}(1)$, one obtains eq 19.²¹ The integration limits ($\phi = 0$ and $\phi = 1$) in eq 19 correspond respectively to a wall with an infinitely strong repulsive nearest neighbor interaction and to a noninteracting wall. Equation 19 was originally used to extract the EoS of a lattice fluid from *NVTMC* simulation data. Here we use it to obtain an alternative route to the EoS within the framework of section 2.1. Results for the wall EoS will be presented in section 4.

3. Monte Carlo Simulations

In previous work^{22,23} we reported *NpTMC* simulations from which the bulk two-particle distributions, $h_{22}(l, m, n)$ and $\omega_2(l, m, n)$, and the EoS of 30 meric cubic lattice fluids

with segmental interaction energies of $u_{\text{attr}} = -0.0k_B T$ and $-0.2k_B T$ were obtained. The simulation method is based on work by Madden³⁶ and considers a polymer slab condensed between a flat wall and a solid piston. Apart from the bulk properties, the method also produces the adsorption profiles of the fluids at the flat wall. Here, we use these profiles for comparison to the adsorption profiles calculated with the polymer-RISM and Scheutjens–Fleer theory. Thus far, only nonattracting walls are considered.

4. Results and Discussion

4.1. Adsorption Profiles. We start by making a few general remarks about the Scheutjens–Fleer (SF) theory.^{7,37,38} It is an extension of the Flory–Huggins mean field lattice theory¹ in which a preaveraging of polymer concentrations in the layers parallel to the adsorbing wall takes place (mean field approximation). All possible molecular conformations are accounted for by a matrix method that calculates the probability of each molecular conformation to occur near the wall. The matrix method accounts for compositional differences between the layers that occur due to the presence of the wall and that propagate via the chain-connectivity and segmental interaction energies.⁷ The SF theory, contrary to the method of section 2.1, allows for conformational changes of the adsorbing molecules. The method is called self-consistent, for the distribution of the molecules over the layers is found by a minimization of the overall free energy of the adsorbing fluid. Its mean field (MF) approximation is physically plausible at higher bulk packing fractions but seems invalid at lower packing fractions. Therefore, it is interesting to compare the SF theory to the approach of section 2.1, which does not adopt a MF approximation. Another reason for us to compare the abilities of the approach of section 2.1 to the SF formalism is the simplicity of the integral equation approach: it only takes solving eq 16 to obtain $g_{12}(l)$ via eq 17, whereas in the SF formalism a coupling of several equations for each layer makes the numerical solution of these equations more complicated.

In this paper, we refer to the original SF formalism,⁷ although more sophisticated versions that use a different discretization of space or partially account for the intramolecular excluded chain volume via a rotational isomeric state (RIS) scheme^{39,40} exist. Note that comparison to the SF formalism that uses a RIS scheme would be more appropriate if the (RF) intramolecular distribution of eq 5 is replaced by a nonreversal random walk (NRRW) intramolecular distribution.

In Figures 1 and 2, some adsorption profiles of linear 30 mer lattice polymeric chains at a noninteracting wall are shown. In Figure 1, $u_{\text{attr}} = -0.0k_B T$ and η_{m2} is 0.2074 (●, and lower lines) and 0.6865 (◆, and upper lines). In Figure 2, $u_{\text{attr}} = -0.2k_B T$ and η_{m2} is 0.2940 (●, lower lines) and 0.7262 (◆, and upper lines). The symbols in the figures are obtained from MC simulations, the dashed lines from the SF theory, and the full lines from the method outlined in section 2.1. We have drawn lines through the calculated profiles to distinguish between theoretical and simulation data.

The MC points in Figures 1 and 2 show a depletion of polymeric molecules near the noninteracting wall in all

(36) Madden, W. G. *J. Chem. Phys.* **1987**, *87*, 1405.

(37) Fleer, G. J.; Cohen Stuart, M. A.; Scheutjens, J. M. H. M.; Cosgrove, T.; Vincent, B. *Polymers at Interfaces*; Chapman and Hall: London, 1993.

(38) Theodorou, D. N. *Macromolecules* **1988**, *21*, 1391.

(39) Leermakers, F. A. M.; Scheutjens, J. M. H. M. *J. Chem. Phys.* **1988**, *89*, 3264.

(40) Flory, P. J. *Statistical Mechanics of Chain Molecules*; Hanser Publishers: Munich, 1989.

(33) Hertanto, A.; Dickman, R. *J. Chem. Phys.* **1988**, *89*, 7577.

(34) McQuarrie, D. A. *Statistical Mechanics*; Harper and Row Publishers: New York, 1976.

(35) Honnell, K. G.; Hall, C. K.; Dickman, R. *J. Chem. Phys.* **1987**, *87*, 664.

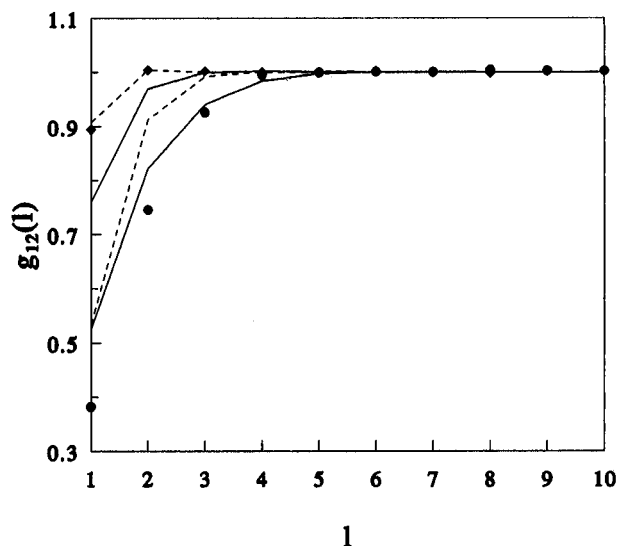


Figure 1. Adsorption profiles of an athermal 30 mer linear chain fluid at a noninteracting wall located at $l = 0$. The bulk packing fractions are $\eta_{m2} = 0.2074$ (●, lower dashed and full line) and 0.6865 (◆, upper dashed and full line). The symbols are obtained from the simulations, the dashed lines from the Scheutjens–Fleer theory, and the full lines from the polymer-RISM theory of section 2.1.

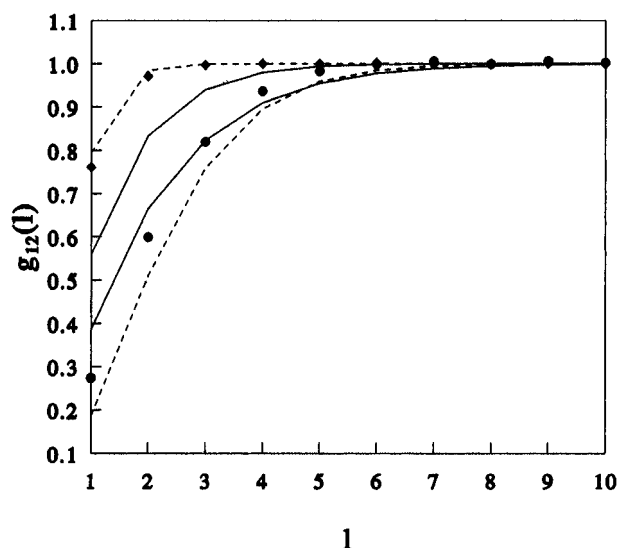


Figure 2. Caption as in Figure 1, but for $u_{\text{attr}} = -0.2k_B T$ with $\eta_{m2} = 0.2940$ (●, lower dashed and full curve) and $\eta_{m2} = 0.7262$ (◆, upper dashed and full line).

four cases. In Figure 1, where results for an athermal fluid near a noninteracting wall are depicted, the depletion is of purely entropic origin: an average segment of a polymeric molecule has a reduced probability of being close to the wall, due to chain-connectivity constraints. In Figure 2, the depletion is increased, when compared to the corresponding packing fractions in Figure 1, due to the cohesive energy of the bulk fluid: apart from the entropic restrictions that the molecules experience in the vicinity of the wall, there is an additional depletion because the wall prevents the molecular segments close to the noninteracting wall to form energetically favorable ($u_{\text{attr}} = -0.2k_B T$) segmental interactions. Note from both figures that the depletion hole is deeper at lower bulk packing fractions: at higher bulk packing fractions the polymeric material is “pushed” to the wall, and in the limit $\eta_{m2} \rightarrow 1$, the simulations will show a completely flat adsorption profile, $g_{12}(l) = 1$ for all l , corresponding to a complete absence of wall–fluid correlations.

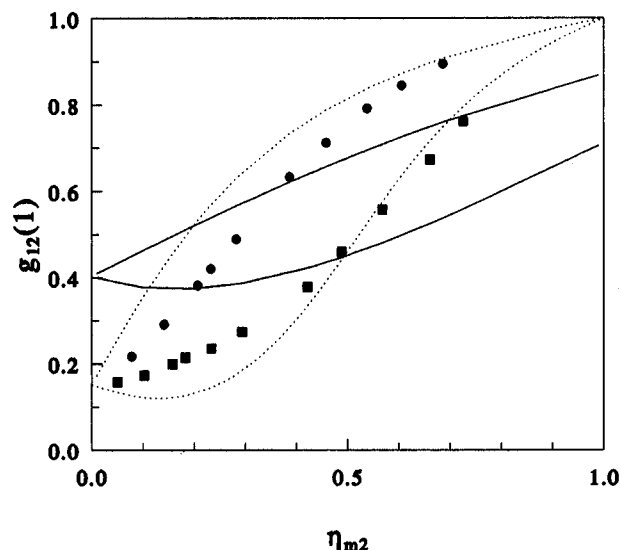


Figure 3. Bulk density dependence of the normalized packing fraction in the layer closest to the nonattracting wall. Full lines are obtained within the polymer-RISM theory and the dotted lines within the SF formalism of ref 7. The symbols are obtained from MC simulation. Circles (●) represent an athermal 30 mer fluid, and boxes (■) a 30 mer fluid with segmental interaction strengths of $u_{\text{attr}} = -0.2k_B T$. Lower full and dotted lines are for the interacting fluid, and upper lines are for the athermal fluid.

From the figures it is seen that the SF theory performs very good at high packing fractions (upper dashed lines), which was to be expected because the MF approximation is most appropriate for dense fluids, and still reasonably well at lower packing fractions (see also Figure 3). The polymer-RISM theory performs less well at high packing fractions: from the upper full lines in Figures 1 and 2 it is seen that for both the athermal fluid and the fluid with $u_{\text{attr}} = -0.2k_B T$, the depletion at the wall is severely overestimated. The absence of possibilities to change the form of the molecules in the interfacial region will certainly be of influence on this failure, but as will become apparent soon, the absence of excluded volume in the RF intramolecular distribution $\hat{\omega}_{2,\text{RF}}(u, v, w)$ is more important. The underestimation of the depletion at the lower packing fractions (lower full lines in Figures 1 and 2 is also due to the use of this deficient $\hat{\omega}_{2,\text{RF}}(u, v, w)$, but before such is discussed we first present an overview of the behavior of the polymer-RISM and SF theory in Figure 3.

In Figure 3, we have plotted the normalized packing fraction in the layer closest to the wall, $g_{12}(l)$, versus the bulk packing fraction, of an athermal (●) and interacting (■, $u_{\text{attr}} = -0.2k_B T$) 30 mer fluid for the polymer-RISM (full lines) and the SF formalism (dotted lines). The symbols are the results of Monte Carlo simulations. The upper full and dotted lines are for the athermal fluid, and the lower full and dotted line are for the interacting fluid.

First, we consider the SF results. It is seen that the η_{m2} dependence of $g_{12}(l)$ displayed by the dotted lines is reasonably accurate for $\eta > 0.5$. The SF theory shows the physically correct full packing limit $g_{12}(l) = 1$ at $\eta_{m2} = 1$. At low packing fraction ($\eta_{m2} < 0.5$) the SF theory is less accurate, although still reasonable. We expect that better results can be obtained by using the RIS scheme of ref 39 or by adopting a higher order MF approximation within the layers.

The predictions of the polymer-RISM theory of section 2.1 (full lines) are further off the simulation results than the SF lines in Figure 3. The full lines clearly show that the dependence of $g_{12}(l)$ on η_{m2} is too weak: the $g_{12}(l)$ is overestimated at low η_{m2} and underestimated at high η_{m2} .

The incorrect high and low density limits of $g_{12}(l)$ in the

polymer-RISM theory are mainly due to the absence of excluded volume in the random flight intramolecular distribution function, $\hat{\omega}_{2,\text{RF}}(u, v, w)$. At high packing fraction this is seen most easily. Due to the occurrence of intramolecular segmental overlaps, there are unoccupied and doubly occupied sites, even if the lattice is fully packed with polymeric molecules. Hence, the sum of the inter- and intramolecular correlations in the bulk of the fluid, $\omega_2(l, m, n) + \eta_{m2} h_{22}(l, m, n)$, is not equal to zero, although this is the physically correct value for a fully packed lattice.²² As a result, there still is a depletion at the wall for $\eta_{m2} = 1$: it is seen from eq 9 that the physically correct adsorption profile $h_{12}(l) = 0$ is only obtained if $\omega_2(l, m, n) + \eta_{m2} h_{22}(l, m, n) = 0$. In ref 22 it was shown that these "rest correlations", the deviations of $\omega_2(l, m, n) + \eta_{m2} h_{22}(l, m, n)$ from 0, at $\eta_{m2} = 1$ can significantly be reduced by using an intramolecular distribution function, $\hat{\omega}_2(u, v, w)$, that (partly) excludes intramolecular segmental overlaps (e.g., the intramolecular distribution of a nonreversal random walk).

At lower packing fractions, the absence of excluded volume in $\hat{\omega}_{2,\text{RF}}(u, v, w)$ is also responsible for the inaccuracy of the polymer-RISM theory. Consider a lattice fluid at bulk packing fraction $\eta_{m2} \rightarrow 0$ near a nonattracting wall. For that case, $g_{12}(l)$ can be expressed with help of eqs 9 and 10 as

$$g_{12}(l) = 1 - \frac{\sum_{m,n} \omega_{2,\text{RF}}(l, m, n)}{\sum_{m,n} \omega_{2,\text{RF}}(0, m, n)} \quad (20)$$

From eq 20 it is seen that $g_{12}(l)$ is fully determined by the bulk intramolecular distribution function. The equation also shows that the adsorption profiles of the athermal and interacting fluid display the same limiting value of $g_{12}(l)$ (full lines in Figure 3), because we have taken the same $\hat{\omega}_{2,\text{RF}}(u, v, w)$ in the calculation of the adsorption profiles of both fluids. Note from Figure 3 that the values of $g_{12}(l)$ calculated from the SF theory do also meet at $\eta_{m2} \rightarrow 0$. In the SF theory, this "single chain adsorption" limit is determined by the wall–fluid interaction. The $g_{12}(l)$ values observed for the simulated fluids also tend to meet at $\eta_{m2} \rightarrow 0$, although slightly different values for $g_{12}(l)$ are expected in the simulations, because the average conformations of isolated interacting and athermal chains are expected to be different. Now, if in eq 20, we replace the random flight intramolecular distribution terms $\omega_{2,\text{RF}}(0, m, n)$ and $\omega_{2,\text{RF}}(1, m, n)$ by the corresponding nonreversal random walk terms $\omega_{2,\text{NRRW}}(0, m, n)$ and $\omega_{2,\text{NRRW}}(1, m, n)$ (see refs 22 and 23 for the calculation of the $\omega_{2,\text{NRRW}}$ terms), we observe a lowering of $g_{12}(l)$ from 0.399 to 0.268. Figure 3 shows that this is a very significant improvement of the polymer-RISM based adsorption theory.

Use of a NRRW intramolecular distribution function instead of a RF intramolecular distribution not only lowers $g_{12}(l)$ at $\eta_{m2} \rightarrow 0$ but also increases $g_{12}(l)$ at $\eta_{m2} = 1$, as already discussed. Therefore, the density dependence of $g_{12}(l)$ is expected to be closer to the η_{m2} dependence observed from the simulations, if a NRRW intramolecular distribution is used in the theory of section 2.1. Thus far we have not undertaken calculations with this improved intramolecular distribution function. In a later stage, it might also be necessary to incorporate the effects of the wall on the average conformation of the molecules.

Before the equation of state results are examined, some words of caution concerning the applicability of the integral equation theory in combination with approximate closures, such as the PY closure used here, are appropriate. For

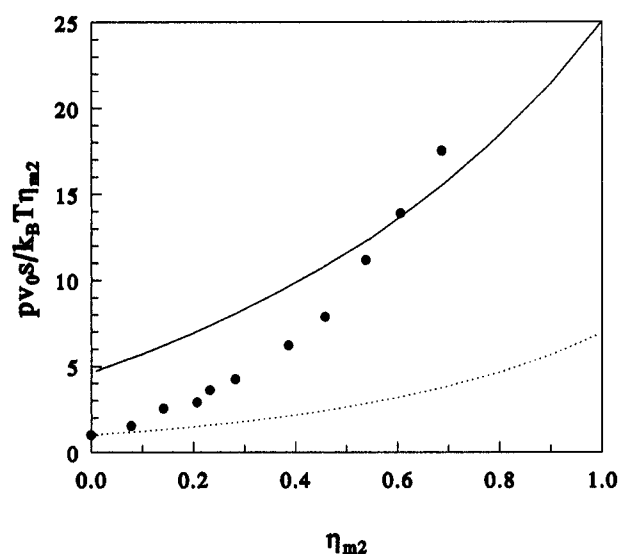


Figure 4. Compressibility factor of an athermal cubic lattice fluid consisting of RF 30 mers. Circles (●) indicate simulation results. The dotted line has been obtained previously via the compressibility-PY route (ref 22). The full line indicates the result obtained via the wall method of section 2.3.

a monatomic continuum fluid, it has been found that at a solid wall the theory is quite successful in the case of athermal fluids. However, in the case of interparticle attractive interactions, the use of the PY approximation leads to the prediction⁴¹ that the contact value at the wall obeys $g_{12}(0) = (\partial \beta P / \partial \eta)^{1/2}$, which can be considerably different from the exact result $g_{12}(0) = \beta P \eta$.⁴² Furthermore it has been demonstrated that integral equation theories in combination with approximate closures, such as the PY one, are unable to account for the complete wetting by liquid occurring at the solid–gas interface or the complete wetting by gas at a purely repulsive substrate at the solid–liquid interface.⁴³ Keeping this in mind one may anticipate similar difficulties with the polymer-RISM theory discussed here. Fortunately, in the case of polymeric fluids the occurrence of the gas–liquid transition is of no real practical consequence and these deficiencies are most likely only of minor importance.

4.2. Equation of State. In this section some results obtained with the wall EoS, eq 19, are presented and compared to MC simulations and to EoS obtained previously from the compressibility–Percus–Yevick (c-PY) and energy–mean spherical approximation (e-MSA) route.^{22,23}

In Figures 4 and 5 we have plotted the compressibility factor $p v_0 s / k_B T \eta_{m2}$ obtained via MC simulation (●), the wall route (full line), the c-PY route (dotted line), and the e-MSA route (dashed line) for a 30 mer fluid with segmental interaction strengths of $u_{\text{attr}} = 0$ (Figure 4), and $-0.2 k_B T$ (Figure 5). The integration over ϕ in the wall-EoS was performed numerically and interpolates between values of $\eta(1) = \eta_{m2} g_{12}(l)$ calculated for 15 wall–fluid interaction strengths varying from $u_{12}(1) \rightarrow \infty$ ($\phi = 0$) to $u_{12}(1) = 0$ ($\phi = 1$). In Figure 4, the e-MSA EoS is not shown, because it reduces to the c-PY EoS in this case of an athermal fluid. The lines depicted in the two figures all use the random flight intramolecular distribution, given by eq 5. Clearly, none of the routes (c-PY, e-MSA, wall) results in an EoS that reasonably reproduces the MC results, although the absolute values of the compressibility factor, $p v_0 s / k_B T \eta_{m2}$ are the best for the wall EoS.

(41) Sullivan, D. E.; Stell, G. *J. Chem. Phys.* **1978**, *69*, 5450.

(42) Fisher, I. Z. *Statistical Theory of Liquids*; University of Chicago: Chicago, IL, 1967.

(43) Evans, R.; Tarazona P.; Marini Bettolo Marconi, U. *Mol. Phys.* **1983**, *50*, 993.

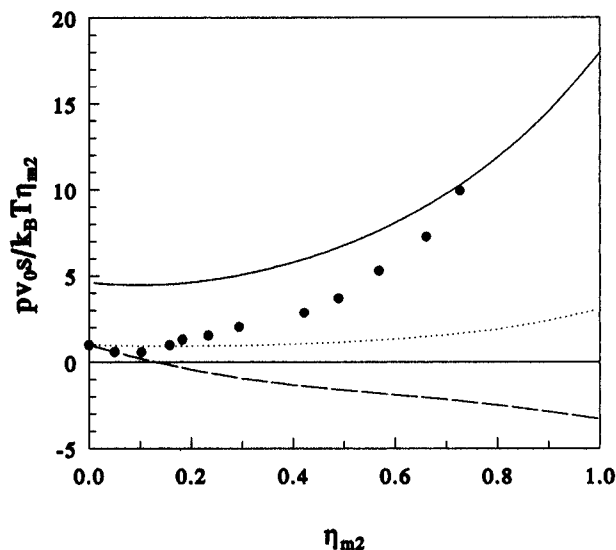


Figure 5. Compressibility factor of a cubic lattice fluid consisting of 30 mer RF chains with segmental interactions of $u_{\text{attr}} = -0.2k_B T$. The circle (●) is obtained from simulations. The dashed and dotted lines indicate results obtained previously via respectively the energy-MSA and compressibility-PY route. The full line indicates the wall EoS obtained via eq 19.

The c-PY and e-MSA EoS have been discussed in detail elsewhere.^{22,23} There it was found that these EoS are extremely sensitive to the exact form of the intramolecular distribution function that is used. The c-PY and e-MSA EoS show the correct ideal gas limit, $p v_0 s / (k_B T \eta_{m2}) = 1$ for $\eta_{m2} \rightarrow 0$. This is in contrast to the wall EoS which, not surprisingly, does not show this limit. This is a result of the absence of excluded chain volume in $\hat{\omega}_{2,\text{RF}}(u, v, w)$. It was shown in the previous subsection that if $\hat{\omega}_{2,\text{RF}}(u, v, w)$ is used, then $g_{12}(l)$ is overestimated at $\eta_{m2} \rightarrow 0$ (see Figure 3). Such will also be the case for a repulsive wall, and hence, the compressibility factor calculated from $g_{12}(l)$ via eq 19 will be overestimated at $\eta_{m2} \rightarrow 0$. Therefore, an improved intramolecular distribution function will certainly lead to an improved compressibility factor at $\eta_{m2} \rightarrow 0$. The physically correct ideal gas limit will not be obtained easily, because in that case $g_{12}(l)$ has to be known exactly. Note from eq 18 that in the case of a monomeric fluid, $g_{12}(l)$ attains the value $g_{12}(l) = e^{-\beta u_{12}(l)}$ in the limit $\eta_{m2} \rightarrow 0$. Thus, insertion of $g_{12}(l)$ in the wall EoS does, in the case of a monomeric fluid, indeed produce the correct ideal gas limit $p v_0 / (k_B T \eta_{m2}) = 1$.

From Figures 4 and 5 it is also seen that the pressure calculated from the wall EoS does not rise to infinity at $\eta_{m2} \rightarrow 1$, again due to the use of $\hat{\omega}_{2,\text{RF}}(u, v, w)$: the physically

correct adsorption profile, $g_{12}(l) = 1$, for which the compressibility factor does go to infinity (see eq 19), will only be obtained if there are no “rest correlations” at $\eta_{m2} \rightarrow 1$, thus if $\omega_2(l, m, n) + \eta_{m2} h_{22}(l, m, n) = 0$ for all (l, m, n) (see eq 9). As shown previously,²² reductions of the “rest correlations”, and thus improvements of the high-density limit of the EoS, are obtained if $\hat{\omega}_{2,\text{RF}}(u, v, w)$ is replaced by $\hat{\omega}_{2,\text{NRRW}}(u, v, w)$. Note from eq 18 that monomeric fluids do again behave correctly at a fully packed lattice: $g_{12}(l) = 1$, and from eq 19 it is then seen that the pressure does rise to infinity for a fully packed monomeric lattice fluid.

5. Conclusions

In this work we have obtained the adsorption profiles of polymeric lattice fluids near an impenetrable wall via a polymer-RISM theory based approach. Calculated profiles for 30 mer fluids near a noninteracting wall have been compared to NpT Monte Carlo simulations and to the Scheutjens–Fleer (SF) theory.⁷ The results of the comparison of both theories to the simulations indicate that the SF theory is more accurate than the polymer-RISM based theory at all packing fractions.

We have also obtained results for the EoS of the bulk fluid from the adsorption profiles.²¹ The EoS results have been compared to simulation results and to previously obtained results based on the compressibility-PY and energy-MSA route.^{22,23}

The absolute values of the compressibility factor obtained via the wall EoS are shown to be an improvement over the values calculated via the compressibility-PY and energy-MSA route, although the wall EoS does not display the correct high and low density limits.

It is shown that the reason for the observed deficiencies of the theory can be largely attributed to the absence of excluded volume in the intramolecular distribution function that was employed. It is made plausible that an improved intramolecular distribution function, e.g., a NRRW scheme, will result in improved adsorption profiles and EoS. Such improvements are straightforward, and since the adsorption profiles obtained from the SF formalism are certainly not perfect (at low density), we think that it is worthwhile to further investigate the method presented here, the more so because it is numerically simple.

Acknowledgment. We like to thank Frans Leermakers from the Department of Physical and Colloid Chemistry of the Wageningen Agricultural University in The Netherlands for the calculation of the adsorption profiles with the Scheutjens–Fleer self-consistent field theory.

LA9608932